J. Fluid Mech. (1992), *vol.* 235, *pp.* 665–689
Printed in Great Britain

On unsteady free convection in vertical slots due to prescribed fluxes of heat or mass at the vertical walls

By FRITZ H. BARK, FARID ALAVYOON AND ANDERS A. DAHLKILD†

Department of Hydromechanics, Royal Institute of Technology, Stockholm, S-10044 Sweden

(Received 7 June 1989 and in revised form 28 August 1991)

Unsteady convection of an initially homogeneous fluid in a vertical slot is investigated theoretically in the limit of large Rayleigh and Prandtl/Schmidt numbers. The motion is driven by prescribed fluxes of heat or mass at the vertical walls of the slot. The 'heat-up' problem is considered, i.e. the fluxes are specified to change instantaneously from zero to finite constant values. Perturbation methods are used to compute approximate solutions for the initial period and for the slow approach to the asymptotic state. Numerical solutions of the full problem are also given. It is shown that a significant stratification is set up after short time and that the system thereafter evolves as a strongly stratified fluid on a timescale that is proportional to $Ra^{\frac{2}{9}}$. During the latter part of the process, linear buoyancy layers of thickness $\sim Ra^{-\frac{2}{9}}$ appear on the vertical walls. On the horizontal walls, there are nonlinear boundary layers of thickness $\sim Ra^{-\frac{1}{9}}$, whose structure is akin to that of a Stewartson $E^{\frac{1}{4}}$ layer. The theoretical predictions are found to be in good agreement with experimental results.

1. Introduction

Theoretical studies of unsteady two-dimensional thermal convection in enclosures where heat is supplied at one of the vertical walls and withdrawn at the other have mainly been concerned with cases where the vertical walls are perfect conductors. A typical problem is to calculate the response of an initially isothermal fluid to an instantaneous change of the temperature of the vertical boundaries. The nonlinear evolution to the steady state was analysed by order of magnitude estimates and computed numerically by Patterson & Imberger (1980). These authors found that the fluid approaches a steady state, which is characterized by boundary layers on the walls and a significant stratification of the density field outside the boundary layers. It was also shown that, under certain circumstances, internal waves appear and that the final steady state thus is approached by an oscillatory motion. These matters were further discussed by Patterson (1983) and investigated experimentally by Ivey (1984). The main features of the mechanism proposed by Patterson & Imberger (1980) for the evolution toward the steady state have been verified by recent accurate numerical simulations by Schladow (1990) and Fusegi, Hyun & Kuwahara (1991). For a detailed account of previous work on the subject, including

† Present address: Department of Gasdynamics, Royal Institute of Technology, Stockholm, S-100 44, Sweden.

experimental work, the reader is referred to the thorough review in Schladow's paper.

Some of the early studies of the steady state in a two-dimensional container with differentially heated walls should be mentioned. The first experiments with cavities having an aspect ratio of order unity were carried out by Eckert & Carlson (1961) whereas vertical slots were studied in the experimental work by Elder (1965). The first theoretical study of the steady state is the work by Batchelor (1954), whose results for the large-Rayleigh-number limit turned out to be at variance with the experiments by Eckert & Carlson (1961). Good agreement with observations were later obtained in the numerical studies by Elder (1966) and de Vahl Davis (1968). The asymptotic structure of the motion in vertical slots for large values of the Rayleigh number has been clarified in the work by Daniels (1987*a*, *b*), which should be consulted for further references.

A closely related class of problems was considered by Hyun (1984, 1985*a*), who computed, by using numerical methods, the response of an initially isothermal fluid in a thermally conducting cylindrical container due to a suddenly imposed constant temperature gradient on the vertical periphery of the container. In qualitative agreement with the results found by Patterson & Imberger (1980) but for a different geometry, Hyun found that internal waves appear during the approach to the steady state. Hyun also discussed the analogous behaviour of the heat-up of a stratified fluid and the spin-up of a homogeneous fluid. For instance, the internal waves in the heat-up case can be said to correspond to the inertial waves that appear during spin-up of a homogeneous fluid, see e.g. Greenspan (1968, p. 38). During nonlinear spin-up, a moving shear front separating regions of different vorticity appears (Greenspan 1968, p. 4). In the problems considered by Hyun (1984, 1985*a*), the corresponding phenomenon is a temperature front separating regions in which there is a rather weak variation of the temperature field.

Several authors have investigated linear problems in which the stratification is regarded as known. In the two-dimensional case, this type of problem is formally completely analogous to the spin-up problem for a rotating homogeneous fluid, see e.g. Veronis (1967*a*, *b*; 1970), Sakurai & Matsuda (1972) and Jischke & Doty (1975). (In the nonlinear cases discussed above, the analogy is only qualitative.) The physical reason for the similar behaviour of the fluid in the two cases is that the permanence of vortex lines in the spin-up case exerts control of the motion in the same way as the stiffening of isopycnic surfaces in the heat-up case. The non-oscillatory part of the motion in spin-up is controlled by Ekman boundary layers on walls that are not parallel with the axis of rotation. In heat-up, the corresponding control is exerted by the buoyancy layers that appear on boundaries that are not perpendicular to the density gradient in the interior of the cavity.

It was shown by Walin (1971) that most of the mathematical difficulties due to nonlinear effects in the heat-up problem disappear if the walls of the container are sufficiently poor conductors. For such cases, Walin was able to derive an approximate but simple linear parabolic equation for the evolution of the density field outside the boundary layers and gave analytic solutions for several cases. Once the solution of Walin's equation for the stratification is known, all properties of the motion can be easily computed analytically to lowest order. Further use of this methodology has been made by Rahm & Walin (1979*a*, *b*). The first of these papers reports a very good agreement between theory and experiments. The same problem as the one considered by Patterson & Imberger (1980) but for a container with walls of finite conductivity has been studied by Rahm (1985), who used an *ad hoc* boundary-layer model to compute the initial set-up of the stratification and Walin's model for the slow approach to the steady state. The heuristic method used by Rahm has been shown to be in acceptable agreement with a numerical solution of the complete problem (Hyun 1985*b*). The physical reason for the success of Walin's approach is that a fluid bounded by poorly conducting walls becomes more strongly stratified than a fluid bounded by efficiently conducting walls. The blocking effect of the strong stratification leads to linear motion in the vertical boundary layers, which makes the mathematical problem tractable by analytic methods.

The heat-up of a fluid in a container with a prescribed heat flux on the walls, which is the subject of the present paper, does not appear to have been considered in the literature. The relevance of this class of problems for thermal engineering has been discussed by Kimura & Bejan (1984). For the steady case, Kimura & Bejan computed an approximate analytical solution for large Rayleigh numbers by using the Oseen-type method proposed by Gill (1966). Also, a numerical solution was computed, which compared well with the approximate analytical solution. One of the problems considered in the present paper is the unsteady version of the large-Prandtl-number limit of the problem considered by Kimura & Bejan (1984).

Another incentive for the present study is need to understand effects of unsteady free convection at large Rayleigh numbers in closed electrochemical systems. Important examples are the unsteady process of charging, or discharging, of batteries with a liquid electrolyte such as the lead acid cell, see e.g. Gu, Nguyen & White (1987). Other applications are electrolytic procedures for refining of metals (Hine 1985). If the electric current density is sufficiently low compared to the limiting current density, which is often the case in applications, the electrode surfaces serve as spatially homogeneous sources or sinks of mass (Awakura, Ebata & Kondo 1979). As the Schmidt number in electrochemical systems is always large, the mathematical model for the heat-up of a fluid of large Prandtl number due to prescribed heat fluxes on the walls is formally the same as that for unsteady electrolysis of a binary electrolyte (Newman 1973).

The paper is organized as follows. The mathematical problem is stated in §2. An approximate analysis of the motion for very small times and an estimate of the time needed to set up a significant stratification are given in §3. In §4, an approximate equation for the slow evolution of the stratification is derived. In contrast to Walin's equation, however, the equation derived in the present work is nonlinear and has to be solved numerically. In order to derive appropriate boundary conditions for the model equation, the horizontal boundary layers have to be considered. These boundary layers, which are discussed in Appendix A, turn out to be very similar to the nonlinear Stewartson $E^{\frac{1}{4}}$ layers appearing in the theory of rotating flows. A brief description of the methodology used in a numerical solution of the complete problem is given in §5. Further details of the numerical method are given in Appendix B. Results are presented and discussed in §6, which also contains a comparison between theoretical predictions and experiments. The main conclusions from the present study are summarized in §7.

2. Problem statement

Consider a two-dimensional vertical slot of height $2L$ and width $2h$. A Cartesian coordinate system (x, z) will be used. The origin of the coordinate system is at the centre of the slot and the z-axis is parallel with the direction of gravity, see figure 1. The slot is filled with a Newtonian fluid. At the vertical walls $x = \pm h$ there are

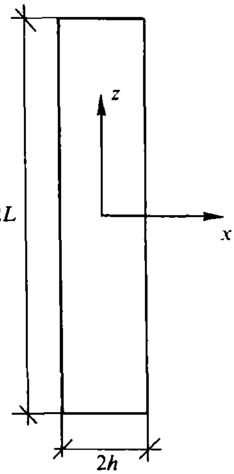

FIGURE 1. Cavity and coordinate system.

prescribed constant fluxes of heat or mass (due to chemical reactions) of magnitude $\kappa A_{\pm}$. The horizontal walls at $z = \pm L$ are assumed to be impenetrable by the flux of heat or mass. In what follows, the mathematical problem will be formulated as a heat transfer problem although, as was pointed out in the introduction, all results apply to the electrolysis of a binary electrolyte for constant electric current densities at the vertical walls. In the Boussinesq approximation, the system of equations to be solved for the velocity field $\boldsymbol{v}$, the pressure field p and the temperature field T if the fluxes $\kappa A_{\pm}$ into the slot are switched on at time $t = 0$ and turned off at $t = t_0$ are

$$\rho(\boldsymbol{v}_t + \boldsymbol{v}\cdot\nabla\boldsymbol{v}) = -\nabla p + \mu\nabla^2\boldsymbol{v} - \rho\alpha(T-T_0)\boldsymbol{g} \tag{1a}$$

$$\nabla\cdot\boldsymbol{v} = 0, \quad T_t + \boldsymbol{v}\cdot\nabla T = \kappa\nabla^2 T, \tag{1b, c}$$

$$\boldsymbol{v} = 0, \quad x = \pm h, \quad |z| \leqslant L, \quad \text{and} \quad |x| \leqslant h, \quad z = \pm L \tag{2a}$$

$$\boldsymbol{e}_x\cdot\nabla T = \pm A_{\pm}[H(t) - H(t-t_0)], \quad x = \pm h, \quad |z| \leqslant L \tag{2b}$$

$$\boldsymbol{e}_z\cdot\nabla T = 0, \quad |x| \leqslant h, \quad z = \pm L. \tag{2c}$$

Here ρ is the density, μ the dynamic viscosity, α the thermal expansion coefficient, T_0 a reference temperature, $\boldsymbol{g}$ the gravitational acceleration, κ the thermal diffusivity and H the Heaviside step function. It should be noted that $\kappa A_{\pm}$ are the fluxes *into* the fluid from the vertical surfaces at $x = \pm h$ and that the magnitudes of these fluxes need not be the same. In thermal problems of the kind considered in this work there is usually no net flux into the cavity because otherwise the solution would, for large values of t_0, eventually become physically unrealistic owing to the occurrence of boiling and other phenomena not accounted for in the mathematical model. However, in mass transfer problems, the fluxes are often of different magnitudes also for cases with large values of t_0. One important example is the lead acid battery. In what follows, the value of t_0 will for simplicity be assumed to be sufficiently large for an asymptotic structure of the solution to develop. The solution will be computed for $t < t_0$.

There are several possible ways of formulating the problem defined by (1*a*)–(2*c*) in non-dimensional form. An obvious choice of temperature scale is Ah with $A =$

max $\{|A_{\pm}|\}$. In problems of the kind considered in this work, the height $2L$ of the slot is usually chosen as the lengthscale as this is the lengthscale over which the forcing is applied. However, the present problem is somewhat unusual in this respect. It will later be shown that, after a short initial period during which a stratification of the fluid is set-up, the motion is controlled by buoyancy layers at the vertical walls in a similar way as a rotating fluid is controlled by Ekman layers, see e.g. Veronis (1970). The dynamics of the buoyancy layers depends on local conditions at the vertical walls and the distance between these. Thus, h is the relevant lengthscale in the present problem. Taking h^2/κ as the timescale and assuming that the dominant force balance is between viscous forces and buoyancy forces, one finds the scales $\rho\alpha A h^3 g/\mu$ and $\rho\alpha A h^2 g$ for velocity and pressure, respectively. The non-dimensional version of (1*a*)–(2*c*) then reads

$$\boldsymbol{v}_t + Ra\, \boldsymbol{v}\cdot\nabla\boldsymbol{v} = Pr(-\nabla\pi + \nabla^2\boldsymbol{v} + T\boldsymbol{e}_z), \tag{3a}$$

$$\nabla\cdot\boldsymbol{v} = 0, \quad T_t + Ra\, \boldsymbol{v}\cdot\nabla T = \nabla^2 T, \tag{3b, c}$$

$$\boldsymbol{v} = 0, \quad x = \pm 1, \quad |z| \leqslant \mathscr{L} \quad \text{and} \quad |x| \leqslant 1, \quad z = \pm\mathscr{L}, \tag{4a}$$

$$\boldsymbol{e}_x\cdot\nabla T = \pm\lambda_{\pm} H(t), \quad x = \pm 1, \quad |z| \leqslant \mathscr{L} \tag{4b}$$

$$\boldsymbol{e}_z\cdot\nabla T = 0, \quad |x| \leqslant 1, \quad z = \pm\mathscr{L}, \tag{4c}$$

where no separate notation has been introduced for the non-dimensional variables. In these equations, T is the non-dimensional temperature deviation, $\mathscr{L}$ the aspect ratio of the cavity and $\lambda_{\pm} = A_{\pm}/A$. The Rayleigh and Prandtl numbers are defined in the usual way, i.e.

$$Ra = \frac{\alpha\rho g A h^4}{\mu\kappa}, \quad Pr = \frac{\mu}{\rho\kappa}.$$

It should be noted that, under conditions such that the present scaling is relevant, a fluid particle will travel a non-dimensional distance of order Ra during a time interval of order unity.

The problem defined by (3*a*)–(4*c*) will be investigated for large values of Ra, Pr and $\mathscr{L}$. Although the full problem appears to be tractable only by using numerical methods, it will be shown in §§3 and 4 that approximate solutions, which are valid outside the end regions, can be found for small and large values of t.

3. Approximate solution for small values of *t*

During the very early stage of the heat-up process, it is reasonable, if $\mathscr{L} \gg 1$ and the Reynolds number $Re = Ra/Pr$ is not too large, to assume that end effects are negligible except for some neighbourhood near the top and bottom of the slot. This motivates the following ansatz:

$$\boldsymbol{v} = w(x,t)\,\boldsymbol{e}_z, \quad p = P(t)\,z, \quad T = T(x,t) \tag{5}$$

for the solution outside the end regions. Substitution of (5) into (3*a*–*c*) and accounting for the boundary conditions (4*a*, *b*) yields

$$v_t = Pr\,(-P(t) + v_{xx} + T), \quad T_t = T_{xx},$$

$$v(\pm 1, t) = 0, \quad T_x(\pm 1, t) = \pm\lambda_{\pm} H(t), \quad v(x,0) = 0, \quad T(x,0) = 0.$$

It should be noted that the Rayleigh number does not appear in the momentum equation under the conditions assumed. An exact solution of the problem for any value of Pr can be readily obtained in terms of Fourier series. The algebraic expressions are, however, a little complicated and are therefore not given here. A physically more transparent solution can be obtained if one makes use of the fact that, for large Prandtl numbers, viscous diffusion is very fast compared to thermal diffusion. This means that, for small values of t, the thermal layers are localized to the neighbourhood of the vertical walls. Moreover, the velocity field is quasi-steady because effects of viscous diffusion have had enough time to spread across the slot. In mathematical terms, this is the limit $Pr \rightarrow \infty$. One can then simply express the temperature and velocity fields in terms of the function

$$\mathscr{T}(x,t) = 2(t/\pi)^{\frac{1}{2}} \mathrm{e}^{-x^2/4t} - x \operatorname{erfc}(x/2t^{\frac{1}{2}}),$$

whereby one obtains

$$T = \lambda_+ \mathscr{T}(1-x,t) + \lambda_- \mathscr{T}(1+x,t) + O(\mathrm{e}^{-1/t}), \tag{6a}$$

$$w = -(\lambda_+ + \lambda_-)\left(\frac{t^{\frac{3}{2}}}{\pi^{\frac{1}{2}}} - \frac{3t^2}{8}\right)(1-x^2) - \int_0^t \{\lambda_+ \mathscr{T}(1-x,t) + \lambda_- \mathscr{T}(1+x,t)\}\,\mathrm{d}t$$
$$- \frac{2t^{\frac{3}{2}}}{3\pi^{\frac{1}{2}}}\{\lambda_+(1+x) + \lambda_-(1-x)\} + O(\mathrm{e}^{-2/t}). \tag{6b}$$

For very small values of t and outside the end regions, one thus finds that the velocity field in the region $|x| < 1 - O(t^{\frac{1}{2}})$, i.e. outside the thermal layers, is the same as that of a homogeneous fluid in a slot, whose horizontal walls are fixed but whose vertical walls at $x = \pm 1$ are moving with the velocities $2\lambda_\pm t^{\frac{3}{2}}/3\pi^{\frac{1}{2}}$. The function $P(t)$ is determined from the condition that the net vertical volume flux in the slot is zero. The solutions ($6a, b$) are compared with a numerical solution of the full problem in figure 2 (a–d). This type of motion is very similar to the steady boundary-layer flow on a heated vertical wall in an isothermal fluid at large Rayleigh and Prandtl numbers investigated by, among others, Le Févre (1957), Ostrach (1963) and Kuiken (1978). Corresponding unsteady cases have recently been investigated by Carey (1983) for a conducting wall and by Carey (1984) for a prescribed flux from the wall. For a more complete review of steady and unsteady boundary layer flows at large Rayleigh and Prandtl numbers, the reader is referred to the book by Gebhart *et al.* (1988, pp. 83–92 and 356–371).

A comment on the validity in time of the solution given by ($6a, b$) may be in order. By assumption, the solution does not account for any effects of stratification. As an estimate of the time needed to set up a significant stratification, it is reasonable to choose the time of travel for a fluid particle that starts in the top region of the slot to reach the bottom region. Taking $w \sim \max\{\lambda_\pm\} t^{\frac{3}{2}}$ according to ($6b$), one finds that the non-dimensional time of travel is of order $(\mathscr{L}/Ra)^{\frac{2}{5}}$. For electrochemical cells, $\mathscr{L}$ is typically of order 10^2 whereas Ra is usually of order 10^5 or more. Thus, the range of validity of the solution given by ($6a, b$) can be expected to be restricted to very small times. It may be worth pointing out that the timescale $(\mathscr{L}/Ra)^{\frac{2}{5}}$ has essentially the same physical meaning as the timescale for the transient leading-edge effect for a suddenly heated vertical plate, see Gebhart *et al.* (1988, p. 355).

A review of convective flows that are geometrically similar to the case discussed in this section can be found in Gebhart *et al.* (1988, pp. 350–354 and 727–733).

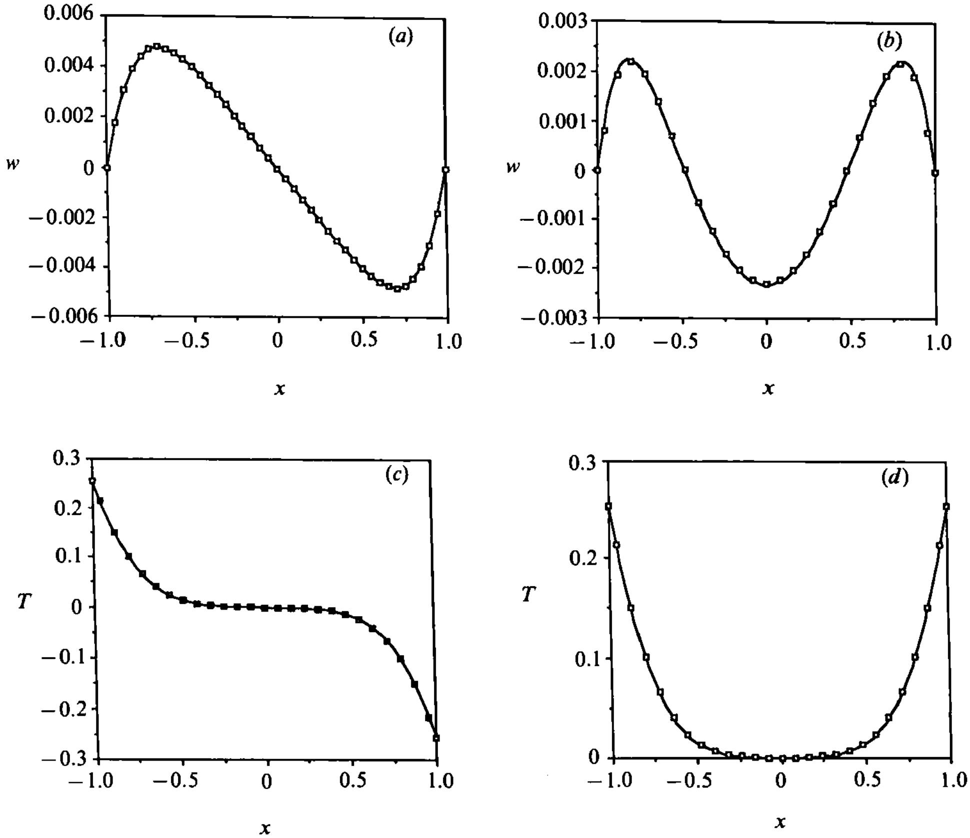

FIGURE 2. (a, b) The vertical velocity component w at $z = 0$ computed from formula (6b) (——) and from numerical solution of the full problem (□). $t = 0.05$, $Ra = 36800$, $Pr = 2100$, $\mathscr{L} = 20$. (a) $\lambda_+ = -\lambda_- = 1$, ($b$) $\lambda_+ = \lambda_- = 1$. ($c$, d) The temperature T at $z = 0$ computed from formula (6a) (——) and from numerical solution of the full problem (□). $t = 0.05$, $Ra = 36800$, $Pr = 2100$, $\mathscr{L} = 20$. (c) $\lambda_+ = -\lambda_- = 1$, ($d$) $\lambda_+ = \lambda_- = 1$.

4. Approximate solution for large times

Under the assumption that end effects are negligible, a matter that will be discussed in some detail later, one may assume that the solution for large values of t asymptotically approaches the following form:

$$\boldsymbol{v} = w(x)\,\boldsymbol{e}_z, \quad \boldsymbol{e}_x \cdot \boldsymbol{\nabla} p = 0, \quad T = \alpha t + S'z + v(x); \quad \alpha, S' \text{ const.} \tag{7}$$

This is a slight generalization of the ansatz made by Prandtl (1952, p. 422) in his model of mountain winds in stratified air, see also Gill (1966).

There are two crucial assumptions embodied in (7). First, it can on reasonable grounds be assumed that the velocity field approaches a steady state for large values of t. As the container is slender, one may expect that this steady velocity field is approximately vertical and depends on x only. Secondly, the temperature field is assumed to consist of three linearly superposed parts: a part αt that grows linearly with time and appears only if there is a net flux of heat into the slot, a linear stratification $S'z$ and a part that depends on x only. This assumption can be briefly justified as follows. If the total heat in the slot increases linearly with t, it is very likely that T will contain a term of the form αt. Because hot (cold) fluid will accumulate in the upper (lower) part of the slot, a stratification will appear. The most simple assumption, which will later be shown to lead to a consistent solution, is to include a linear stratification in the ansatz. One must also account for the horizontal heat fluxes at the vertical walls. This is done by including the term $\upsilon(x)$ in the expression for T.

Some simplifications result if one introduces a redefined reduced pressure $\Pi = p-\alpha zt-\frac{1}{2}S'z^2$. Substitution of (7) into (3*a*, *b*) and the boundary conditions (4*a*) gives the following problem:

$$-\Pi_z+w''+\upsilon = 0, \quad \alpha+S'Ra\; w = \upsilon'', \tag{8a, b}$$

$$w(\pm 1) = 0, \quad \upsilon'(1) = \lambda_+, \quad \upsilon'(-1) = -\lambda_-. \tag{9}$$

As the pressure p, by assumption, is independent of x, (8*a*) shows that Π_z is a constant. In order to compute $w(x)$ and $\upsilon(x)$ from these equations one must thus determine the three unknown constants Π_z, α and S'. Integrating (8*b*) across the slot and noting that the vertical net volume flux is zero gives

$$\alpha = \tfrac{1}{2}(\lambda_+ + \lambda_-). \tag{10}$$

Additional conditions are needed to determine S' and Π_z. S' is determined by the fact that the slot is closed by thermally insulated walls at $z = \pm\mathscr{L}$. If an asymptotic solution of the form (7) is approached for large t, one must require that the vertical net transport of heat at any value of z is zero in order to avoid a physically unreasonable accumulation of heat in the end regions (cf. Bejan 1979), i.e.

$$\int_{-1}^{1}(-T_z+Ra\, wT)\,\mathrm{d}x = \int_{-1}^{1}(-S'+Ra\, w\upsilon)\,\mathrm{d}x = 0. \tag{11a}$$

Π_z is determined from the condition of global conservation of heat, i.e.

$$\int_{-1}^{1}\int_{-\mathscr{L}}^{\mathscr{L}}\mathscr{T}\,\mathrm{d}z\,\mathrm{d}x = 4\alpha t\mathscr{L}+\int_{-1}^{1}\int_{-\mathscr{L}}^{\mathscr{L}}\upsilon\,\mathrm{d}z\,\mathrm{d}x = t\int_{-\mathscr{L}}^{\mathscr{L}}[\upsilon'(1)-\upsilon'(-1)]\,\mathrm{d}z \tag{11b}$$

which, in view of (9) and (10), can be simplified to

$$\int_{-1}^{1}\int_{-\mathscr{L}}^{\mathscr{L}}\upsilon\,\mathrm{d}z\,\mathrm{d}x = 0. \tag{11c}$$

It turns out to be convenient to introduce the notation $\beta = (\frac{1}{4}S'Ra)^{\frac{1}{4}}$. For large values of β, the boundary-layer solution of (8*a*, *b*) and (9) reads

$$\begin{aligned}\upsilon-2\mathrm{i}\beta^2 w = \Pi_z + 1/\beta[\lambda_+\,\mathrm{e}^{-\beta(1+\mathrm{i})(1-x)}+\lambda_-\,\mathrm{e}^{-\beta(1+\mathrm{i})(1+x)}]\\ +(\lambda_+ + \lambda_-)/4\beta^2\,[\mathrm{i}-(1+\mathrm{i})\{\mathrm{e}^{-\beta(1+\mathrm{i})(1-x)}+\mathrm{e}^{-\beta(1+\mathrm{i})(1+x)}\}].\end{aligned} \tag{12}$$

As expected, one finds that the motion takes place mainly in buoyancy layers at the vertical walls. For $\lambda_+ \neq -\lambda_-$ there is also a weak inviscid motion in the interior.

The quantity S' can now be determined from (11*a*) and (12). For large values of Ra, the result is approximately

$$S' = 4\,Ra^{-\frac{1}{9}}\left(\frac{\lambda_+^2+\lambda^2}{128}\right)^{\frac{4}{9}} - \frac{2^{\frac{5}{3}}Ra^{-\frac{3}{9}}(\lambda_+ + \lambda_-)^2}{9(\lambda_+^2+\lambda_-^2)^{\frac{2}{3}}} + O(Ra^{-\frac{5}{9}}), \tag{13}$$

which implies that the thickness of the buoyancy layers $\beta^{-1} \sim Ra^{-\frac{2}{9}}$. It should be pointed out that the solution given by (12) and (13) is an exact solution of the Navier–Stokes equations. The boundary conditions are fulfilled with an error $\sim e^{-2\beta}$, which, for large Ra, is very small. For $\lambda_+ = -\lambda_- = 1$, one recovers the analytical solution obtained by Kimura & Bejan (1984) but here derived in perhaps a little more direct way. The expression for Π_z, which is readily calculated from (11c) and (12), is not needed in what follows and is therefore not given.

The next step is to assume that the pressure gradient and the stratification, which in the previous development were labelled Π_z and S', are slowly varying functions in space and time and to derive evolution equations for these quantities. Formula (13) shows that a new lengthscale $\sim Ra^{\frac{1}{8}}$ appears in the z-direction. Guided by this result, it appears natural to use $\epsilon = Ra^{-\frac{1}{8}}$ as the small parameter in a perturbation scheme. One finds that a meaningful perturbation problem of multiple-scale type can be formulated if one introduces the slow variables $\zeta = \epsilon z$ and $\tau = \epsilon^2 t$ and the ansatz (7) is generalized to

$$\left.\begin{aligned} T &= \alpha t - \mathscr{S}(\zeta,\tau;\epsilon) + \epsilon^2 \mathscr{t}(\mathscr{S},\eta;\epsilon) + \dots, \\ \boldsymbol{v} &= \epsilon^6 \mathscr{w}(\mathscr{S},\eta;\epsilon)\,\boldsymbol{e}_z + \epsilon^9 \mathscr{u}(\mathscr{S},\eta;\epsilon)\,\boldsymbol{e}_x + \dots, \\ \Pi_z &= \epsilon^4 \mathscr{P}_z(\mathscr{S};\epsilon) + \dots, \end{aligned}\right\} \tag{14}$$

where $\eta = \epsilon^{-2}(1 \pm x)$, α is given by formula (10) and the functions $\mathscr{S}$, $\mathscr{t}$, $\mathscr{w}$, $\mathscr{u}$ and $\mathscr{P}_z$ are assumed to be of order unity. The reason why a parametric dependence on ϵ has been assumed for these quantities will be discussed in a moment. It should be noted that the functions $\mathscr{t}$, $\mathscr{w}$ and $\mathscr{u}$, which are assumed to have boundary-layer character, depend on $\mathscr{S}(\zeta,\tau)$ but not explicitly on either t or τ. This means that, on the timescale considered, the boundary-layer fields are assumed to adjust instantaneously to the current value of $\mathscr{S}$. The corresponding (very accurate) approximation in spin-up problems is that, on the spin-up timescale for a homogeneous fluid, the Ekman layers adjust immediately to the geostrophic flow. An important consequence of the scaling assumed in (14) is that the order of magnitude of the vertical diffusive transport of heat in the interior is the same as that of the net vertical advective transport. It can be shown that the ansatz (14) leads to a consistent approximation outside the end regions if $Pr \gg Ra^{-\frac{1}{8}}$.

Approximate expressions for $\mathscr{t}$ and $\mathscr{w}$ (in terms of $\mathscr{P}_z$) can be obtained from (12) by taking $S' = \epsilon \mathscr{S}_\zeta$ and solving for $v = \epsilon^2 \mathscr{t}$ and $w = \epsilon^6 \mathscr{w}$. Once $\mathscr{w}$ is known, $\mathscr{u}$ can be computed from the equation of continuity. $\mathscr{P}_z$ can be computed from (11b). It should be pointed out that this perturbation procedure does not give the same results as would have been obtained from a formal expansion of all variables in powers of ϵ^2. However, the results differ only in the $O(\epsilon^2)$ correction for the buoyancy layers. A straightforward but somewhat tedious analysis shows that this difference has no consequences for the results in what follows. The heuristic approach used in this work turns out to be algebraically much more simple than a formal expansion scheme.

An equation for $\mathscr{S}$ can be obtained by considering the heat balance in a slab between ζ and $\zeta + \Delta\zeta$, i.e.

$$\int_{-1}^{1}\int_{\zeta}^{\zeta+\Delta\zeta} \mathscr{S}_\tau(\zeta',\tau)\,\mathrm{d}x\,\mathrm{d}\zeta = \int_{-1}^{1} [\mathscr{S}_\zeta(\zeta+\Delta\zeta,\tau) - \mathscr{S}_\zeta(\zeta,\tau)$$

$$+ \epsilon^{-2}\{\mathscr{w}\mathscr{t}(\zeta+\Delta\zeta,\tau) - \mathscr{w}\mathscr{t}(\zeta,\tau)\}_\zeta]\,\mathrm{d}x,$$

which is correct to $O(\epsilon^2)$. It should be noted that the terms wt are of order unity only in the buoyancy layers, which means that the term that is multiplied by ϵ^{-2} in the right-hand side results in a term of order unity. Substitution of w and t, being computed in terms of $\mathscr{S}_\zeta$ as outlined above, leads, after some algebra, in the limit $\Delta\zeta \rightarrow 0$ to the following nonlinear parabolic equation for $\mathscr{S}$:

$$\mathscr{S}_\tau = \left[1 + \frac{5\sqrt{2}}{32}(\lambda_+^2 + \lambda_-^2)\,\mathscr{S}_\zeta^{-\frac{9}{4}} - \frac{3\epsilon^2}{8}(\lambda_+ + \lambda_-)^2\,\mathscr{S}_\zeta^{-\frac{5}{2}}\right]\mathscr{S}_{\zeta\zeta} + O(\epsilon^4). \tag{15}$$

Apart from the somewhat trivial solution $\mathscr{S} = \text{const.} \times \zeta + \text{const.}$, which, as will be discussed below, is of some relevance in the present problem, no analytic solution of this equation has been found. However, the equation is much easier by far to solve numerically than the complete problem (3*a*)–(4*c*). As $\mathscr{S}$ is computed numerically from (15), there is no reason to expand $\mathscr{S}$ in powers of ϵ^2 and compute different terms separately. The next issue to be considered is the specification of boundary and initial conditions for $\mathscr{S}$.

The boundary conditions at $\zeta = \pm\epsilon\mathscr{L} = \pm\mathscr{H}$, say, follow from consideration of the horizontal boundary layers that appear at the top and bottom of the slot. (For the analysis in the rest of the paper, the order of magnitude of $\mathscr{H}$ need not be specified.) Some details of these boundary layers are discussed in Appendix A. One finds that the boundary-layer thickness is ϵ and the assumption of negligible end effects is thus valid as long as $\mathscr{L} \gg \epsilon = Ra^{-\frac{1}{5}}$. The mathematical structure of the boundary-layer problem is, as could be expected, quite similar to that for the nonlinear Stewartson $E^{\frac{1}{4}}$ layer that appears during spin-up of a homogeneous fluid. It is shown in Appendix A that the motion in the horizontal boundary layers is independent of τ to the order considered. This means that the conservation constraint expressed by (11), and hence (13), must be used as the matching condition for $\mathscr{S}$ to the solution in the horizontal boundary layers. The boundary conditions for the solution of (15) can thus be stated directly as

$$\mathscr{S}_\zeta = \mathscr{S}_{0\zeta} = 4\left(\frac{\lambda_+^2 + \lambda_-^2}{128}\right)^{\frac{4}{9}} - \frac{2^{\frac{5}{3}}\epsilon^2(\lambda_+ + \lambda_-)^2}{9(\lambda_+^2 + \lambda_-^2)^{\frac{2}{3}}}, \quad \zeta = \pm\mathscr{H}. \tag{16}$$

In view of these boundary conditions, it appears reasonable to infer, and this will be verified later, that the solution of (15) for large values of τ asymptotically approaches the exact steady solution

$$\mathscr{S} = \mathscr{S}_{0\zeta}\,\zeta. \tag{17}$$

The initial condition for the solution of (15) cannot be formulated by matching to the solution obtained in the previous section simply because there is no intermediate limit in which the two solutions are asymptotically the same. The physical reason for this is that the solution (6*a*, *b*) does not account for any effects of stratification whereas, in the derivation of (15), such effects are assumed to control the motion. Somewhat fortunately, it turns out that $\mathscr{S}$ can be computed quite accurately from (15) without detailed knowledge of the proper matching condition for small values of τ. The reason is that the 'diffusivity' in (15) is $\sim \mathscr{S}_\zeta^{-\frac{9}{4}}$ to lowest order in ϵ^2 for small values of $\mathscr{S}_\zeta$. In the problem under consideration the stratification $\mathscr{S}_\zeta$ starts to build up from zero, which means that the diffusivity will, for small values of τ, be very large. From a numerical point of view, this is a favourable situation as the solution will become essentially independent of the details of the initial conditions after a

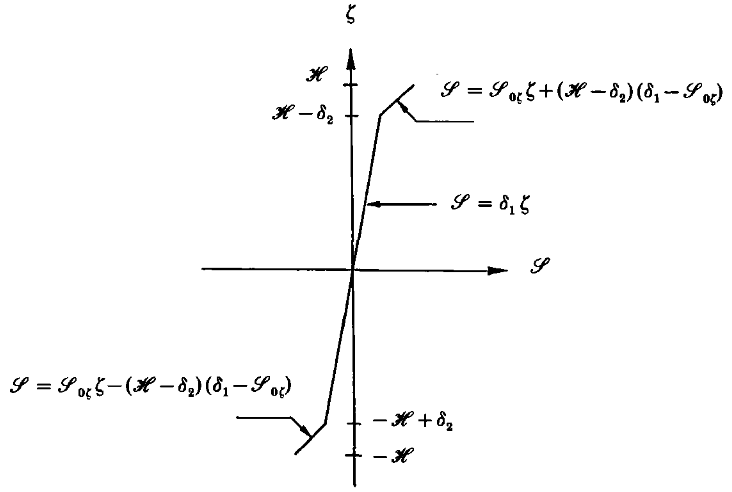

FIGURE 3. *Ad hoc* initial condition for equation (15).

short time. Specifically, consider a Fourier representation of the (unknown) matching condition for small values of τ. Equation (15) shows that a Fourier component of wavelength ℓ will decay on a timescale of order $\ell^2\mathscr{S}_{\zeta}^{\frac{9}{4}}$, which means that small scale variations decay very rapidly. Guided by this observation, extensive numerical experiments were carried out with *ad hoc* initial conditions of the form (see figure 3)

$$\mathscr{S}(\zeta,0)=\delta_1\zeta,\quad |\zeta|\leqslant\mathscr{H}-\delta_2, \tag{18a}$$

$$\mathscr{S}(\zeta,0)=\mathscr{S}_{0\zeta}\zeta\pm(\mathscr{H}-\delta_2)(\delta_1-\mathscr{S}_{0\zeta}),\quad 0\leqslant|\mathscr{H}\pm\zeta|\leqslant\delta_2, \tag{18b}$$

where δ_1 and δ_2 are small positive numbers. It was consistently found that the results were very insensitive to the particular choice of the numerical values of δ_1 and δ_2. Also, continuous functions having the property (16) and similar shape to (18*a*, *b*) were tried with the same result. It should be pointed out that the details of the short initial period during which the stratification is set up are in most practical cases of significantly less interest than those of the long-time evolution of the system.

Some comments on the physical mechanism that is responsible for the large diffusive effects for small values of τ may be in order. It has already been pointed out that vertical transport of heat due to molecular diffusion and advection are both included in the derivation of (15). The advective transport, which takes place mainly in the buoyancy layers, is accounted for by the terms that contain inverse functional fractional powers of $\mathscr{S}_{\zeta}$. If $\mathscr{S}_{\zeta}$ is small, i.e. the stratification is weak, the motion in the buoyancy layers will be strong and the advective part of the transport is significantly stronger than that due to molecular diffusion. In (15), a strong advective transport then appears as a large diffusivity $\sim\mathscr{S}_{\zeta}^{-\frac{9}{4}}$.

Solutions of the approximate problem will be given in §6 after the method for numerical solution of the complete problem has been outlined.

5. Numerical method for the solution of the full problem

In terms of the stream function ψ and the vorticity $\omega = (\boldsymbol{e}_x \times \boldsymbol{e}_z)\cdot(\boldsymbol{\nabla}\times\boldsymbol{v})$, equations (3$a$, b) and the boundary condition (4a) read

$$\omega_t + Ra\,\boldsymbol{\nabla}\cdot\omega\boldsymbol{v} = Pr(\nabla^2\omega + T_x), \tag{19a}$$

$$\nabla^2\psi = -\omega, \tag{19b}$$

$$\psi = 0, \quad x = \pm 1, \quad |z| \leqslant \mathscr{L} \quad \text{and} \quad z = \pm\mathscr{L}, \quad |x| \leqslant 1, \tag{20a}$$

$$\psi_x = -w = 0, \quad x = \pm 1, \quad |z| \leqslant \mathscr{L}, \tag{20b}$$

$$\psi_z = u = 0, \quad z = \pm\mathscr{L}, \quad |x| \leqslant 1. \tag{20c}$$

Equations (19a, b) and (3c) were solved numerically with the boundary conditions (20a–c) and (4b, c) using a slightly modified version of a scheme developed by Johansson (1987). The scheme is second-order accurate in time and space. The convective and diffusive terms are approximated by the Leapfrog and Crank–Nicolson schemes respectively. For the details of the discretized equations and boundary conditions, see Appendix B.

The discretized equations and boundary conditions define two linear systems of algebraic equations to be solved at each time level. The matrix elements of the systems are constants and are computed once and for all at the start of a computation. The system of equations is solved by using the Gauss–Seidel method with successive relaxation.

The properties of the scheme have been analysed mathematically by Johansson (1987). Resolution of the vertical and horizontal boundary layers requires the spatial mesh (in the boundary layers) to be of order $Ra^{-\frac{2}{9}}$ in the horizontal direction and $Ra^{-\frac{1}{9}}$ in the vertical direction. In the computations presented in this work, a Cartesian mesh, uniform in each coordinate direction, was chosen for reasons of simplicity and flexibility. For such a mesh, fulfilling the minimum space resolution requirements, it was shown by numerical experiments that the time step must be of order Ra^{-1} for the scheme to be stable. This led to quite time-consuming executions of the program.

6. Discussion of results

In this section some results are presented for the cases of odd and even forcing. In the odd case one has $\lambda_+ = -\lambda_- = -1$, which corresponds to the thermal problem considered by Kimura & Bejan (1984) or an antisymmetric electrochemical system such as electrolysis of a binary electrolyte. The even case, in which $\lambda_+ = \lambda_- = 1$, is an idealized system that has been chosen for its simplicity. Batteries with a liquid electrolyte are in general a compromise between the cases of odd and even forcing, which, of course cannot be superposed. In all cases discussed in this section, the higher-order corrections in (15), (16) are deleted.

The perturbation solution derived in §4, is, from a formal point of view, valid for $\epsilon \ll 1$ and $\tau = \epsilon^2 t = O(1)$ or larger, i.e. for large values of t. However, it is a fortunate circumstance that the perturbation solution turns out to be numerically quite accurate not only for values of ϵ that are not extremely small but also for $t \sim 1$. In order to illustrate these matters, some comparisons between perturbation solutions and numerical solutions of the full problem are shown in figure 4(a–c). These graphs

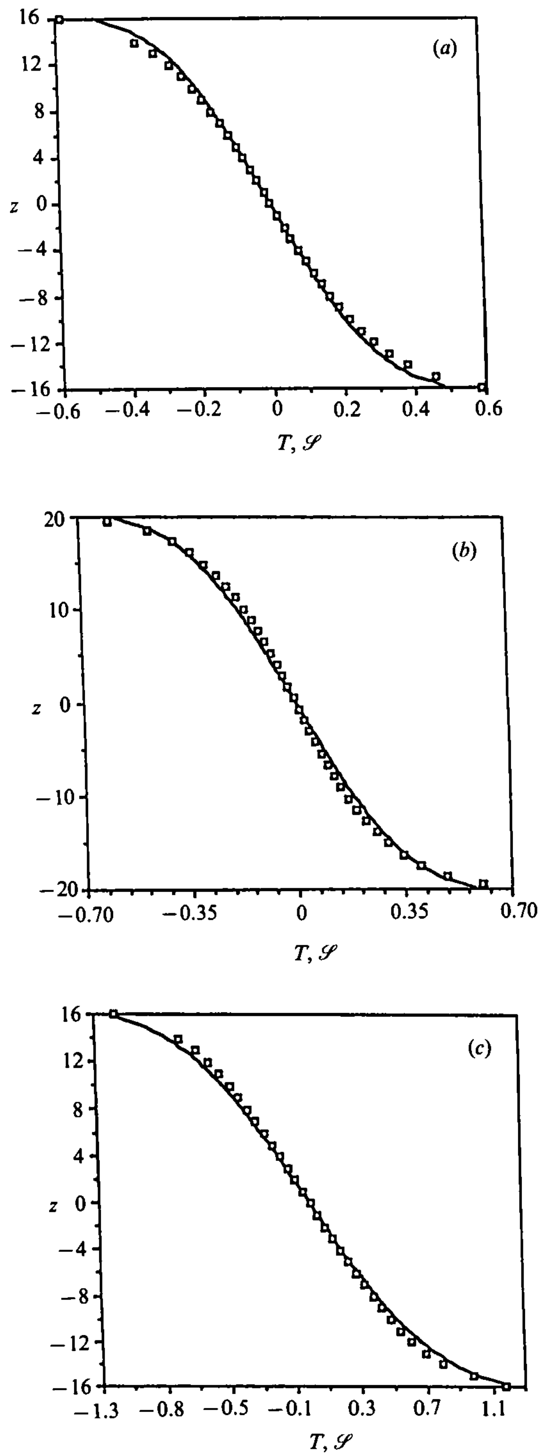

FIGURE 4. Comparison between the function $\mathscr{S}$ (—) computed from equation (15) and T for $x = 0$ (□) from the numerical solution of the full problem for: (*a*) $\epsilon = 0.266$, $t = \epsilon^{-2}\tau = 0.4$, $Ra = 147200$, $Pr = 2100$, $\mathscr{L} = 16$, $\lambda_+ = -\lambda_- = 1$; (*b*) $\epsilon = 0.311$, $t = \epsilon^{-2}\tau = 0.5$, $Ra = 36800$, $Pr = 2100$, $\mathscr{L} = 20$, $\lambda_+ = -\lambda_- = 1$; (*c*) $\epsilon = 0.493$, $t = \epsilon^{-2}\tau = 1.0$, $Ra = 575$, $Pr = 2100$, $\mathscr{L} = 16$, $\lambda_+ = -\lambda_- = 1$.

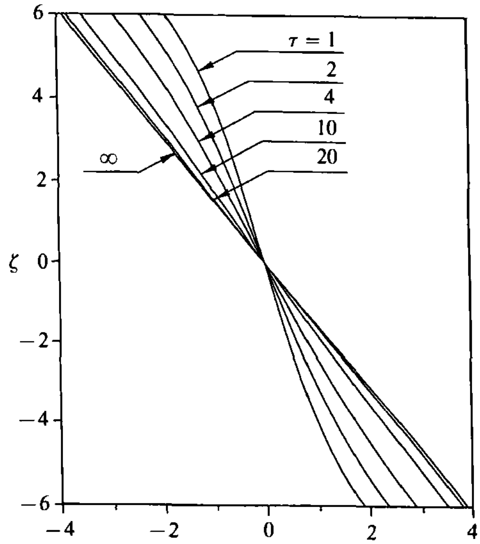

FIGURE 5. Evolution of the solution $\mathscr{S}(\zeta, \tau)$ of equation (15) towards the asymptotic state. $\epsilon = 0.311$, $\lambda_+ = -\lambda_- = 1$.

show $\mathscr{S}(\zeta, \tau)$ and $T(0, z, t)$ in the case of odd forcing, where the latter is obtained from the numerical solution of the full problem, for three values of the Rayleigh number (147200, 36800, 575) for three different values of t (0.4, 0.5, 1). For each of the Rayleigh numbers, the respective values of t have been chosen as small as possible while retaining good agreement between $\mathscr{S}(\zeta, \tau)$ and $T(0, z, t)$. For all values of Ra, the agreement becomes better (worse) for larger (smaller) values of τ. Figure 4(c) shows that the approximate perturbation solution is quite accurate for $\epsilon \approx 0.5$, which is not extremely small. It is also obvious from figure 4(a–c) that the perturbation solution is a good approximation for $t \sim 1$, which is outside its formal range of validity. The approach of $\mathscr{S}$ to the steady-state solution given by (17) is shown in figure 5. Note that the solution obtained by solving (8a, b) with the boundary conditions (9) is an exact solution of the Navier–Stokes equations for any Prandtl number. This implies that the asymptotic solution for the evolution of the stratification $\mathscr{S}$ will presumably work for any Prandtl number after a sufficiently long time. However, as the numerical solution of the full problem becomes a much more difficult issue for $Pr \sim 1$ or smaller, we have so far been unable to validate this assertion.

The evolution of the system in the odd case is illustrated in figures 6(a–c) and 7(a–c), which show streamlines and isotherms, respectively, for representative values of τ. It should be noted that the values of $\Delta\psi$ are not the same in figures 6(a)–6(c). The velocity is largest during the initial phase when effects of blocking due to stratification are insignificant. Even though the value of τ in figure 6(a) is only a small fraction of the diffusion time based on the distance between the vertical walls, end effects are obviously felt in the whole slot. This is consistent with the conclusion drawn in §3 that the ends of the slot will affect the motion after a very short time. In figures 6(b) and 7(b), it can be seen that the vertical and horizontal boundary layers and the stratification are reasonably distinct for $\tau = 0.3$. Even though the system for this value of τ is quite far from its asymptotic state, see figure 5, the stratification is sufficiently strong for the perturbation theory given in §4 to give very

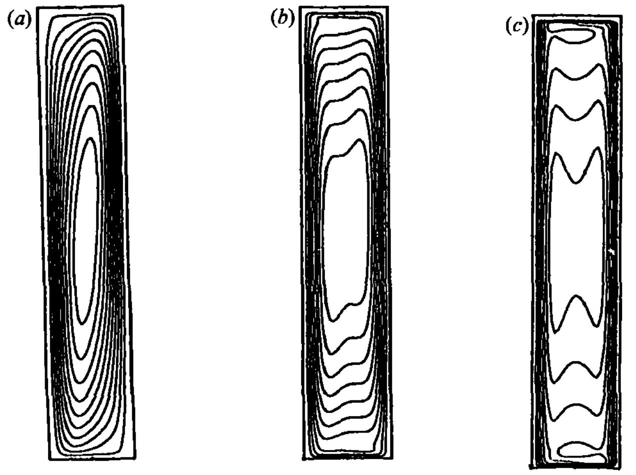

FIGURE 6. Streamlines for different values of t computed numerically from the full problem. $Ra = 36800$, $Pr = 2100$, $\mathscr{L} = 20$, $\lambda_+ = -\lambda_- = 1$, $\epsilon = 0.311$. (*a*) $t = \epsilon^{-2}\tau = 0.2$, $\psi_{min} = -3.18 \times 10^{-3}$, $\psi_{max} = -3.18 \times 10^{-4}$, $\Delta\psi = 3.7 \times 10^{-5}$; (*b*) $t = \epsilon^{-2}\tau = 3$, $\psi_{min} = -6.6 \times 10^{-4}$, $\psi_{max} = -3.18 \times 10^{-5}$, $\Delta\psi = 2.6 \times 10^{-5}$; (*c*) $t = \epsilon^{-2}\tau = 30$, $\psi_{min} = -2.65 \times 10^{-4}$, $\psi_{max} = -2.6 \times 10^{-5}$, $\Delta\psi = 1.7 \times 10^{-5}$.

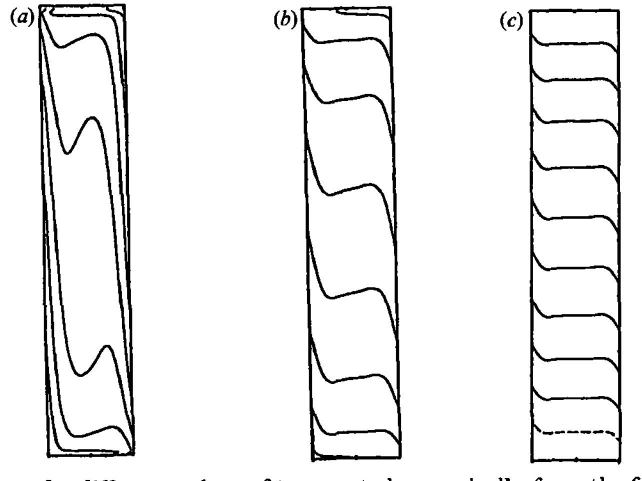

FIGURE 7. Isotherms for different values of t computed numerically from the full problem. (*a*) $t = \epsilon^{-2}\tau = 0.2$, $T_{min} = -0.987$, $T_{max} = 0.400$, $\Delta T = 0.154$; (*b*) $t = \epsilon^{-2}\tau = 3$, $T_{min} = -1.94$, $T_{max} = 1.26$, $\Delta T = 0.356$; (*c*) $t = \epsilon^{-2}\tau = 30$, $T_{min} = -2.19$, $T_{max} = 2.22$, $\Delta T = 0.490$. Ra, Pr, $\mathscr{L}$, λ_+, λ_- and ϵ are the same as in figure 6.

accurate results. For $\tau > 3$, the geometry of streamlines and isotherms changes very little. The level curves for ψ and T shown in figures 6(*c*) and 7(*c*) are thus close to those of the asymptotic state.

Comparisons between results obtained from perturbation theory and numerical solution of the full problem are shown in figure 8(*a*, *b*). These graphs show the vertical velocity component and the temperature field in the odd case as functions of x at the mid-height of the cavity for a small value of τ. The agreement is good and becomes, as was pointed out before, even better for larger values of τ.

Streamlines and isotherms for three values of τ for the case of even forcing are shown in figures 9(*a*–*c*) and 10(*a*–*c*). These results were obtained from the numerical

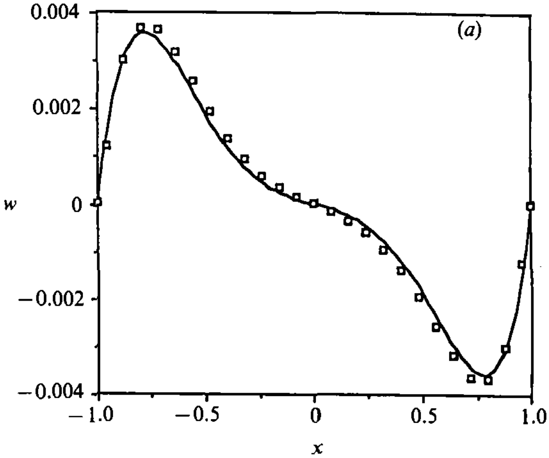

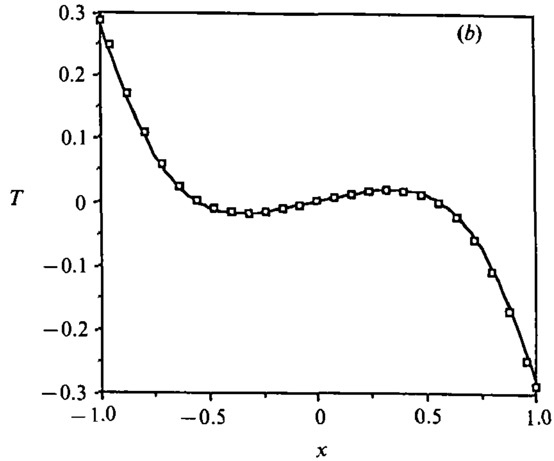

FIGURE 8. (*a*) The vertical velocity component w and (*b*) the temperature T at $z = 0$ computed from perturbation theory (——) and from numerical solution of the complete problem (□). $t = \epsilon^{-2}\tau = 0.5$, $\epsilon = 0.311$, Ra, Pr, $\mathscr{L}$, λ_+ and λ_- are the same as in figure 6.

solution of the full problem. In figure 11, the vertical velocity component and the concentration fields computed from the perturbation theory are compared with the corresponding results from the numerical solution of the full problem. The agreement is quite good but not as good as in the odd case, cf. figure 8(*a*, *b*). As the accuracy of the perturbation solution depends on the strength of the stratification, this means that the time needed to set up a significant stratification outside the buoyancy layers is somewhat larger in the even case. This effect can also be observed by comparing figure 6(*b*) with figure 9(*b*). The boundary-layer character of the motion is more pronounced in figure 6(*b*).

It is noteworthy that the size of the end regions is very much smaller than in the case with isothermal vertical walls considered by Elder (1965). In the present case with prescribed fluxes at the vertical walls, the end regions are boundary layers of thickness $\sim Ra^{-\frac{1}{8}}$. In the case considered by Elder, where effects of stratification are weaker, the influence of the horizontal walls extend a distance $\sim Ra$ along the slot (Daniels 1985) which can be considered as an 'end region' only if $\mathscr{L} \gg Ra$.

Several authors, see e.g. Fusegi *et al.* (1991), have demonstrated that the approach to the asymptotic state in heat-up problems, under certain circumstances, is

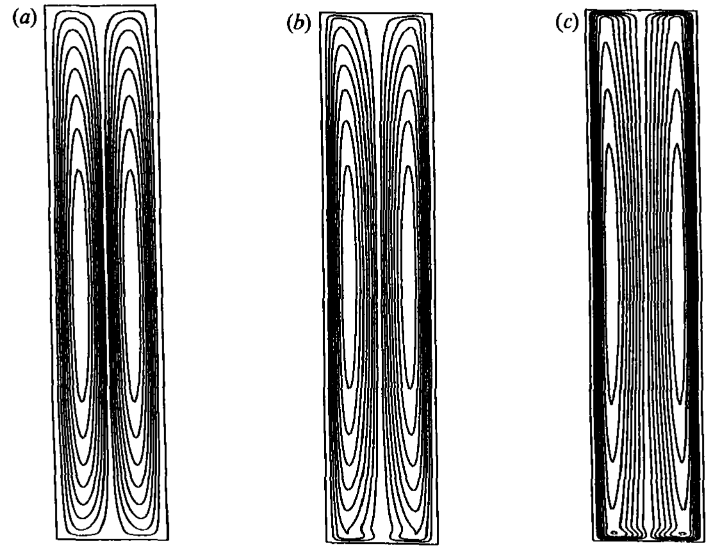

FIGURE 9. Streamlines for different values of t computed numerically from the full problem. $Ra = 36800$, $Pr = 2100$, $\mathscr{L} = 20$, $\lambda_+ = \lambda_- = 1$, $\epsilon = 0.311$. (*a*) $t = \epsilon^{-2}\tau = 0.2$, $\psi_{min} = 0$, $\psi_{max} = 1.54 \times 10^{-3}$, $\Delta\psi = \frac{1}{9}\psi_{max}$; (*b*) $t = \epsilon^{-2}\tau = 3$, $\psi_{min} = 0$, $\psi_{max} = 4.3 \times 10^{-4}$, $\Delta\psi = \frac{1}{9}\psi_{max}$; (*c*) $t = \epsilon^{-2}\tau = 30$, $\psi_{min} = 0$, $\psi_{max} = 1.79 \times 10^{-4}$, $\Delta\psi = \frac{1}{9}\psi_{max}$.

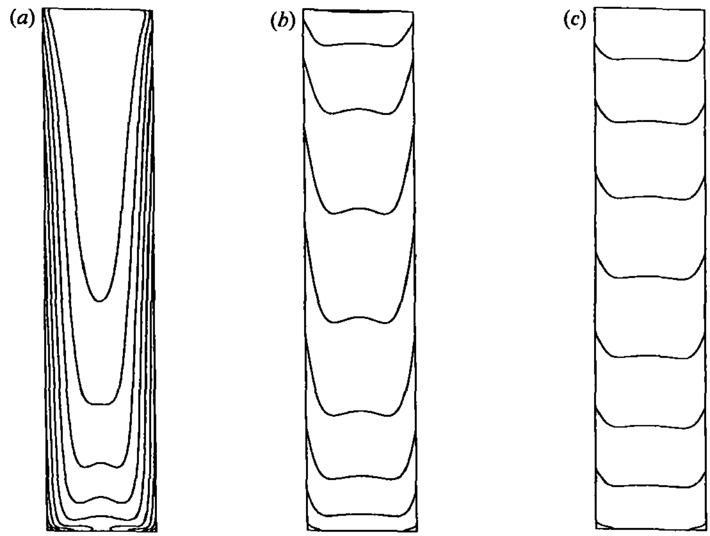

FIGURE 10. Isotherms for different values of t computed numerically from the full problem. (*a*) $t = \epsilon^{-2}\tau = 0.2$, $T_{min} = 0.1$, $T_{max} = 0.65$, $\Delta T = 0.0688$; (*b*) $t = \epsilon^{-2}\tau = 3$, $T_{min} = 2.03$, $T_{max} = 4.1$, $\Delta T = 0.259$; (*c*) $t = \epsilon^{-2}\tau = 30$, $T_{min} = 27.3$, $T_{max} = 3.18$, $\Delta T = 0.563$. Ra, Pr, $\mathscr{L}$, λ_+, λ_- and ϵ are the same as in figure 9.

oscillatory. These oscillations are internal waves. No internal waves were detected in the numerical computations reported on in the present work. The reason is simply that such waves are dissipated very rapidly by viscous forces. This matter may be worth a few comments. Assuming for the sake of simplicity that there are no effects of boundaries and taking the stratification to be given by (17), it is a straightforward matter to compute the frequency of an internal wave from the linearized versions of

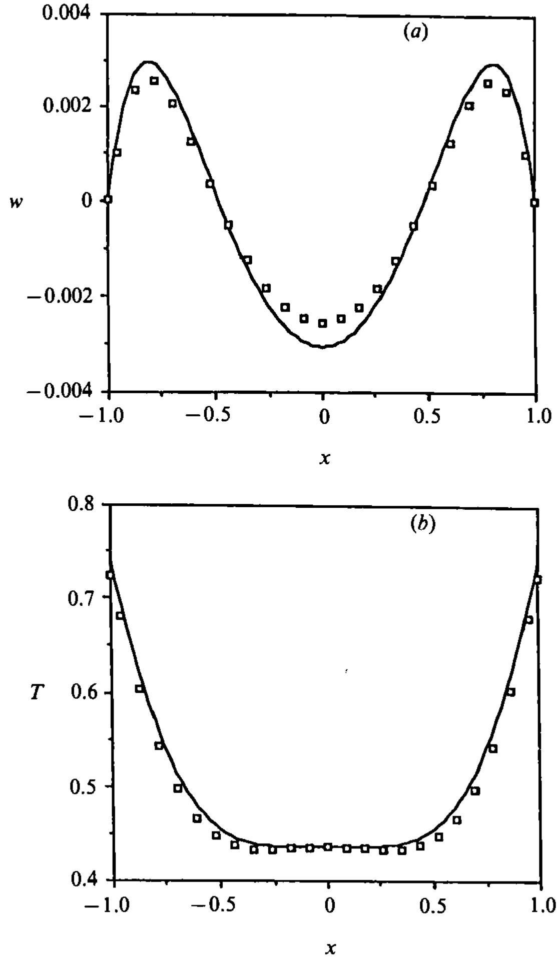

FIGURE 11. (*a*) The vertical velocity component w and (*b*) the temperature T at $z = 0$ computed from perturbation theory (——) and from numerical solution of the full problem (□). $t = \epsilon^{-2}\tau = 0.5$, $\epsilon = 0.311$, $\lambda_+ = \lambda_- = 1$. Ra, Pr, $\mathscr{L}$ are the same as in figure 9.

(3*a–c*). If the velocity, reduced pressure and temperature fields are represented by expressions of the form

$$(v, \pi, T) = (V, \Pi, T) \exp\left[\mathrm{i}(\omega t + k_x x + k_z z)\right],$$

where the quantities V, Π and T are constants, one finds, under the assumption that

$$Ra^{\frac{8}{9}} \mathscr{S}_{0\zeta}/Pr \gg 1,$$

the following approximate expression for the frequency:

$$\omega = \pm\{k_x^2 \, Pr \, Ra^{\frac{8}{9}} \mathscr{S}_{0\zeta}/k^2\}^{\frac{1}{2}} + \tfrac{1}{2}\mathrm{i}k^2 Pr, \tag{21}$$

with $k = (k_x^2 + k_z^2)^{\frac{1}{2}}$. The first term in (21) is the Brunt–Väisälä frequency and the second term is the decay rate. Consequently, internal waves having wavelengths of the same order of magnitude as the distance between the vertical walls can be expected to have a decay rate that is proportional to the Prandtl number, which in the present work is assumed to be large. It should be remembered that the assumption that effects of boundaries are negligible makes (21) correct only as an order of magnitude estimate.

Comparisons between predictions of the perturbation theory developed in the

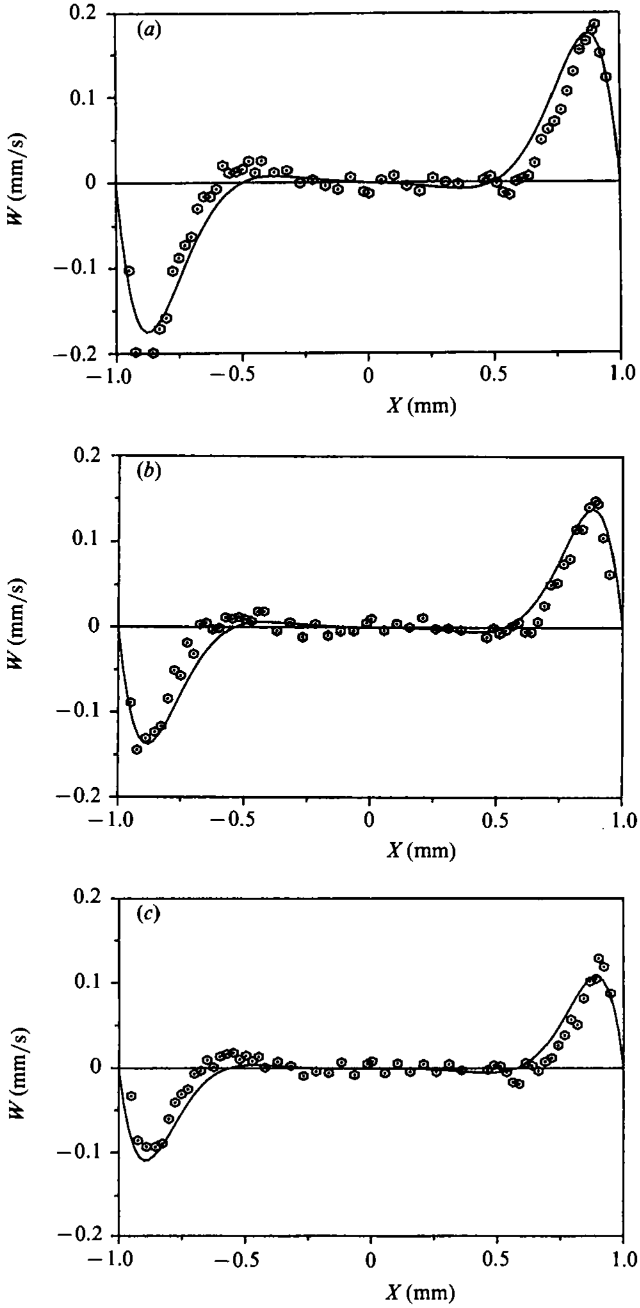

FIGURE 12. Comparison of w at cavity mid-height ($z = 0$) from the experiments by Karlsson *et al.* in a copper cell and the asymptotic theory (——); $Ra = 308000$. (*a*) $t = 15$ min ($\tau = 0.045$), (*b*) $t = 30$ min ($\tau = 0.09$), (*c*) $t = 60$ min ($\tau = 0.18$).

present work and experimental results are available in the literature. The development in time of the vertical velocity field in the electrochemical system Cu(s)/$CuSO_4$(aq)/Cu(s) has been measured by Karlsson, Alavyoon & Eklund (1990). Figure 12(*a–c*), which is taken from that work, shows that the agreement between theory and experiment is good. The evolution of the vertical variation of the

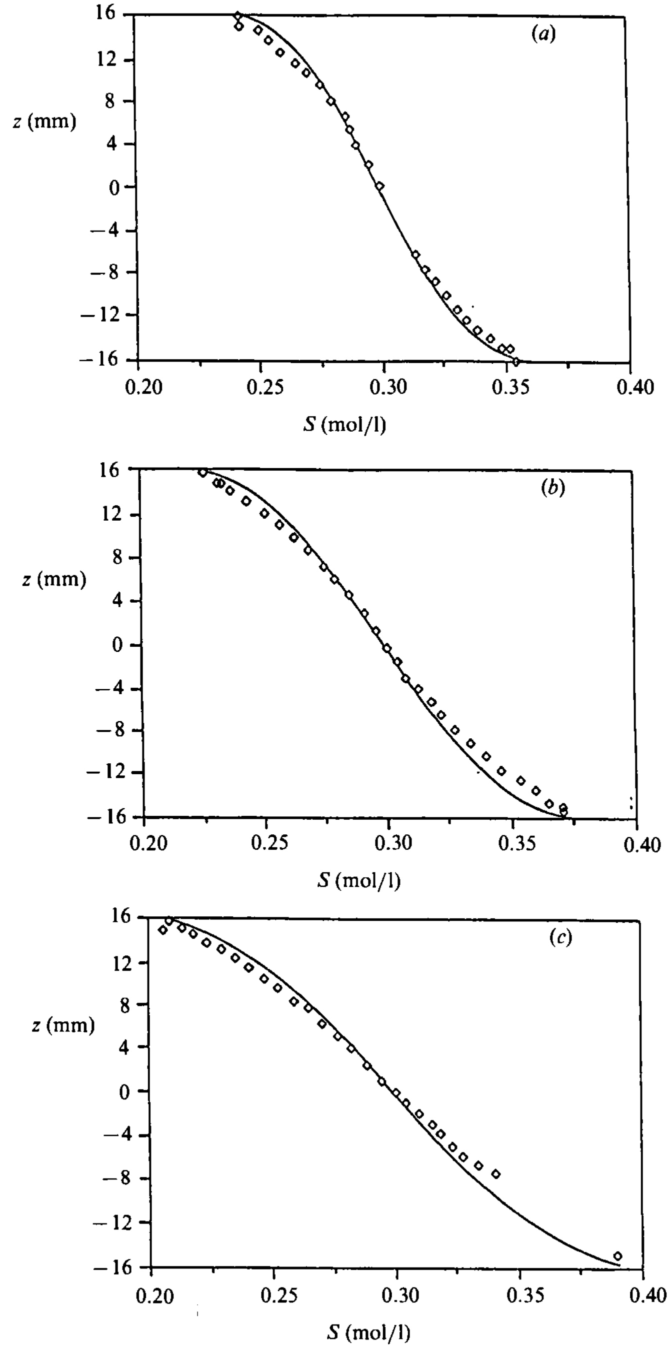

FIGURE 13. Comparison of the stratification from the experiments by Eklund *et al.* and the asymptotic theory (——), $Ra = 308000$. (*a*) $t = 15$ min ($\tau = 0.045$), (*b*) $t = 30$ min ($\tau = 0.09$), (*c*) $t = 60$ min ($\tau = 0.18$).

concentration field in the mid-section of the electrochemical cell, i.e. $c(0, z, t)$, has been measured by Eklund *et al.* (1991). Owing to the boundary-layer character of the concentration field, $c(0,z,t) \approx \mathscr{S}(\zeta, \tau)$ to a high degree of accuracy outside the horizontal boundary layers. Figure 13 (*a–c*), which is taken from the paper by Eklund *et al.* (1991), shows that the theoretical results are in good agreement with experiments for the concentration field also. The perturbation theory is thus validated by comparisons with both experiments and numerical solutions of the full problem.

7. Summary of results and methodology

The unsteady convective motion of an initially homogeneous fluid in a vertical slot due to suddenly imposed fluxes of heat (or mass) at the vertical walls of the slot has been considered for large values of the Rayleigh and Prandtl/Schmidt numbers. It has been shown that effects of stratification become of importance after a time period of order $(\mathscr{L}/Ra)^{\frac{2}{5}}h^2/\kappa$, where $\mathscr{L}$ and h are the aspect ratio and the half-width of the slot, respectively, Ra the Rayleigh number and κ the heat (or mass) diffusivity. The initial part of the 'heat-up' process, is, in practical cases, usually very short.

After the stratification has been established, the velocity and concentration fields evolve on the slow timescale $h^2/Ra^{\frac{2}{9}}\kappa$ toward an asymptotic state, in which the density field outside the boundary layers has a linear variation in the vertical direction. During this phase of the process, the motion is strongly blocked by the stratification. There are linear buoyancy layers of thickness $Ra^{-\frac{2}{9}}h$ on the vertical walls and nonlinear boundary layers of thickness $Ra^{-\frac{1}{9}}h$ on the horizontal walls. The latter layers are quite similar to the nonlinear Stewartson $E^{\frac{1}{4}}$ layer that appears on vertical walls during the spin-up of a homogeneous fluid. In analogy with the spin-up problem, there is presumably also a thinner boundary layer of thickness $Ra^{-\frac{4}{27}}h$ nested within the aforementioned horizontal layer but this matter has not been investigated in this work. Outside the boundary layers, there is a weak inviscid motion, whose strength compared to that of the motion in the buoyancy layers is of order $Ra^{-\frac{2}{9}}$.

The asymptotic structure of the motion for large Rayleigh and Prandtl/Schmidt numbers was investigated by using perturbation methods. An approximate analytic solution was computed for the initial phase before the stratification is established. For the slow approach to the asymptotic state, an approximate partial differential equation for the evolution of the density field outside the boundary layers was derived. The boundary conditions for this equation could be determined from a simple analysis of the problem for the motion in the horizontal boundary layers. The formulation of the initial condition turned out to be much more difficult because there is no region of overlap with the solution for short times. Therefore, the initial condition had to be formulated on an *ad hoc* basis. Very fortunately, the solution turned out to depend surprisingly weakly on the details of the initial condition, even for small times referred to the long timescale $h^2/Ra^{\frac{2}{9}}\kappa$. Once the interior density field has been computed numerically, all quantities outside the horizontal boundary layers can be simply calculated analytically.

The complete problem was solved by numerical methods. The results were found to be in good agreement with those obtained from perturbation theory. It turned out that the numerical solution of the complete problem was quite time-consuming. The perturbation approach, which requires considerably less computational efforts, may thus be useful in applications.

Theoretical predictions from the perturbation theory developed in the present work were found to be in very good agreement with measurements of the velocity field by Karlsson *et al.* (1990) and the concentration field by Eklund *et al.* (1991) in an electrochemical cell.

Most of the numerical computations leading to the results reported on in the present work were carried out by the third author at the IBM Scientific Centre in Rome. The authors are very grateful for the generous support to the present work from the IBM company. In particular, the authors would like to thank Dr P. Sguazzero of the Italian IBM company and Dr L. Arosenius and B. Sc. E. Weibust of the Swedish IBM company. The authors are much obliged to Professor B. Gustafsson, Dr G. Amberg and Dr C. Johansson for several discussions about the numerical method outlined in §5.

Appendix A

In this Appendix, some properties of the boundary layers on the horizontal walls are discussed and a possible solution procedure for the mathematical problem is outlined. The purpose of the outline is to demonstrate that the problem for the horizontal boundary layers appears to be well posed, which, in addition to the results derived in §4, is a quite strong indication that the solution of the complete problem in the limit of large Prandtl and Rayleigh numbers indeed has an asymptotic structure of the assumed form.

In the boundary-layer problem for the motion near the bottom of the slot, a stretched coordinate $\xi = \epsilon^{-1}(\mathscr{L}+z)$ is defined and the dependent variables are represented as follows:

$$\left.\begin{aligned} T &= \alpha t - \mathscr{S}(-\mathscr{H}) + \epsilon^2 \mathscr{t} + \dots, \quad w = \epsilon^8 \mathscr{w} + \dots, \quad u = \epsilon^7 \mathscr{u} + \dots, \\ p &= \epsilon(\mathscr{S}(-\mathscr{H}) - \alpha t)\,\xi + \epsilon^3 \mathscr{p} + \dots . \end{aligned}\right\} \tag{A 1}$$

Substitution of (A 1) into ($3a$–c) leads to the problem

$$0 = -\mathscr{p}_\xi - \mathscr{t}, \quad 0 = -\mathscr{p}_x, \quad \mathscr{w}\mathscr{t}_\xi + \mathscr{u}\mathscr{t}_x = \mathscr{t}_{\xi\xi}, \quad \mathscr{w}_\xi + \mathscr{u}_x = 0. \tag{A 2a–d}$$

To lowest order, the boundary layer is thus quasi-steady and hydrostatic. It follows from (A $2a$, b) that $\mathscr{t}$ does not depend on x. Hence, the second term on the left-hand side of (A $2c$) drops out and it follows that $\mathscr{w}$ is also independent of x. One then finds from (A $2d$) that $\mathscr{u}$ is linear in x. In principle, $\mathscr{u}$ can thus be computed in terms of $\mathscr{t}$ from matching to the solutions in the buoyancy-layer extensions in the regions $|\xi| \sim 1, |\eta| = |\epsilon^{-2}(1 \pm x)| \sim 1$. These regions will be briefly discussed below. If $\mathscr{u}$ is known, $\mathscr{w}$ can be computed by integration of (A $2d$). The constant of integration is determined by matching to the interior part of the vertical velocity $\mathscr{w}$. Once $\mathscr{w}$ is known in terms of $\mathscr{t}$, (A $2c$) becomes a nonlinear second-order ordinary differential equation for $\mathscr{t}$. It seems very reasonable to impose the following boundary and matching conditions for the solution of this equation:

$$\mathscr{t}_\xi = 0, \quad \xi = 0; \qquad \lim_{\xi \to \infty} \mathscr{t} = -\mathscr{S}_{0\zeta}\,\xi. \tag{A 3a, b}$$

The formally incorrect notation for the limit in (A $3b$) is here used as an abbreviation for the algebraically somewhat complicated intermediate limit process described, for example, in the book by Cole (1968, p. 9). Using the definition of ξ in terms of ζ, one finds that T, for large values of ξ, behaves as

$$T = \alpha t - \mathscr{S}(-\mathscr{H}) - \mathscr{S}_{0\zeta}(\mathscr{H}+\zeta) + \dots,$$

which is the inner behaviour of the outer solution. The matching can thus, in principle, be carried out to lowest order. The mathematical structure of the problem defined by (A $2a$–d) and (A $3a$, b) is very similar to that of the problem for nonlinear Stewartson $E^{\frac{1}{4}}$ layers in the theory of rotating fluids (Bennets & Hocking 1973; Smith 1981).

In the buoyancy-layer extensions, the dependent variables are expressed as

$$\left.\begin{aligned} &T = \alpha t - \mathscr{S}(-\mathscr{H}) + \epsilon^2 \mathscr{t}_B + \ldots, \quad w = \epsilon^6 \mathscr{w}_B + \ldots, \quad u = \epsilon^7 \mathscr{u}_B + \ldots, \\ &p = \epsilon(\mathscr{S}(-\mathscr{H}) - \alpha t)\,\xi + \epsilon^3 \mathscr{p}_B + \ldots, \end{aligned}\right\} \tag{A 4}$$

which leads to the following system of equations:

$$0 = -\mathscr{p}_{B\xi} + \mathscr{w}_{B\eta\eta} - \mathscr{t}_B, \quad 0 = -\mathscr{p}_{B\eta}, \quad \mathscr{w}_B \mathscr{t}_{B\xi} + \mathscr{u}_B \mathscr{t}_{B\eta} = \mathscr{t}_{B\eta\eta}, \quad \mathscr{w}_{B\xi} + \mathscr{u}_{B\eta} = 0. \tag{A 5a–d}$$

Equation (A 5*b*) implies that $\mathscr{p}_B = \mathscr{p}$. One then finds from (A 2*a*) that (A 5*a*) can be written

$$\mathscr{w}_{B\eta\eta} - \mathscr{t}_B + \mathscr{t} = 0. \tag{A 5e}$$

From (A 5*e*) one can, in principle, compute $\mathscr{w}_B(\eta,\xi)$ in terms of $\mathscr{t}_B$ and $\mathscr{t}$. The two arbitrary functions of ξ that appear as constants of integration are determined from the boundary conditions

$$\mathscr{w}_B(0,\xi) = \mathscr{w}_B(\infty,\xi) = 0. \tag{A 6}$$

One can thereafter compute $\mathscr{u}_B(\eta,\xi)$ by solving (A 5*d*) subject to the boundary condition

$$\mathscr{u}_B(0,\xi) = 0, \tag{A 7}$$

which means that $\mathscr{u}$ can be computed by matching to $\mathscr{u}_B$. The coefficients $\mathscr{w}_B$ and $\mathscr{u}_B$ in (A 5*c*) are now, in principle, known in terms of $\mathscr{t}_B$ and $\mathscr{t}$. This equation can thus be written as an integro-differential equation of parabolic type for $\mathscr{t}_B(\eta,\xi)$. It seems reasonable to infer that this equation can be solved subject to the boundary and matching conditions

$$\mathscr{t}_{B\eta}(0,\xi) = \lambda_\pm, \quad \lim_{\substack{\eta\to\infty \\ \xi\ \text{fixed}}} \mathscr{t}_B = \mathscr{t}, \quad \lim_{\substack{\xi\to\infty \\ \eta\ \text{fixed}}} \mathscr{t}_B = -\mathscr{S}_{0\zeta}\xi + \mathscr{t}(\eta). \tag{A 8a–c}$$

The solution of the perturbation problem outlined above would require extensive and certainly quite difficult numerical computations.

It is readily shown that the neglected terms $\mathscr{t}_\tau$ and $\mathscr{t}_{B\tau}$ in (A 2*c*) and (A 5*c*) are of order ϵ^4 and ϵ^6, respectively, compared with the terms retained. It is therefore consistent to impose the boundary condition (13) for the solution of (15) even if the term of order ϵ^2 on the right-hand side of that equation is kept.

There are still boundary conditions that are not corrected by the solution of the problem discussed above. In analogy with the spin-up problem, there is very likely a thinner layer of thickness $\epsilon^{\frac{4}{3}}$, which would correspond to the Stewartson $E^{\frac{1}{3}}$ layer, as well as $\epsilon^2 \times \epsilon^2$ corner regions. The mathematical problems to be solved in these regions are not discussed in this work.

Appendix B

The discretized version of the equations and the boundary conditions (19*a*, *b*), (3*c*), (20*a–c*) and (4*b*, *c*) read

$$\frac{\omega^{n+1}_{i,j} - \omega^{n-1}_{i,j}}{2\Delta t} + Ra\,\{D_{0x}(u^n_{i,j}\,\omega^n_{i,j}) + D_{0z}(w^n_{i,j}\,\omega^n_{i,j})\}$$
$$= Pr\,\{\tfrac{1}{2}\nabla^2_0(\omega^{n+1}_{i,j} + \omega^{n-1}_{i,j}) + D_{0x}T^n_{i,j}\}, \quad 2 \leqslant i \leqslant M-1, 2 \leqslant j \leqslant N-1; \tag{B 1}$$

$$\nabla^2_0 \psi^{n+1}_{i,j} = -\omega^{n+1}_{i,j}, \quad 1 \leqslant i \leqslant M, 1 \leqslant j \leqslant N; \tag{B 2}$$

$$\frac{T^{n+1}_{i,j} - T^{n-1}_{i,j}}{2\Delta t} + Ra\,\{D_{0x}(u^n_{i,j}\,T^n_{i,j}) + D_{0z}(w^n_{i,j}\,T^n_{i,j})\}$$
$$= \tfrac{1}{2}\nabla^2_0(T^{n+1}_{i,j} + T^{n-1}_{i,j}), \quad 1 \leqslant i \leqslant M, 1 \leqslant j \leqslant N; \tag{B 3}$$

$$\psi_{i,j} = 0, \quad i = 0,1,M,M+1, 0 \leqslant j \leqslant N+1, \quad j = 0,1,N,N+1, 0 \leqslant i \leqslant M=1; \tag{B 4}$$

$$T_{0,j} = T_{1,j} + \lambda_- \Delta x, \quad 1 \leqslant j \leqslant N; \tag{B 5}$$

$$T_{M+1,j} = T_{M,j} + \lambda_+ \Delta x, \quad 1 \leqslant j \leqslant N; \tag{B 6}$$

$$T_{i,1} = T_{i,0}, \quad 1 \leqslant i \leqslant M; \tag{B 7}$$

$$T_{i,N+1} = T_{i,N}, \quad 1 \leqslant i \leqslant M. \tag{B 8}$$

Here $D_{0x,z}$ are the discretized centred derivative operators in the x- and z-directions, respectively. ∇_0^2 is the discretized Laplace operator. M and N are the number of grid points in the x- and z-directions. Equations (B 1), (B 2), (B 4) and (B 3), (B 5)–(B 8) define two linear systems of algebraic equations with constant coefficient matrices. Equation (B 1) lacks boundary conditions and therefore (B 2) is used for defining the values of $\omega_{i,j}$ in terms of $\psi_{i,j}$ on the boundaries.

REFERENCES

Awakura, Y., Ebata, A. & Kondo, Y. 1979 *J. Electrochem. Soc.* **126**, 23.

Batchelor, G. K. 1954 *Q. J. Appl. Maths* **12**, 209.

Bejan, A. 1979 *J. Fluid Mech.* **71**, 729.

Bennets, D. A. & Hocking, L. M. 1973 *Proc. R. Soc. Lond.* A **333**, 469.

Carey, V. P. 1983 *Intl J. Heat Mass Transfer* **26**, 911.

Carey, V. P. 1984 *Intl J. Heat Mass Transfer* **27**, 419.

Cole, J. D. 1968 *Perturbation Methods in Applied Mathematics.* Blaisdell.

Daniels, P. G. 1985 *Intl J. Heat Mass Transfer* **28**, 2071.

Daniels, P. G. 1987*a* *J. Fluid Mech.* **176**, 419.

Daniels, P. G. 1987*b* *Q. J. Appl. Maths* **40**, 257.

Eckert, E. R. & Carlson, W. O. 1961 *Intl J. Heat Mass Transfer* **2**, 206.

Eklund, A., Alavyoon, F., Simonsson, D., Karlsson, R. I. & Bark, F. H. 1991 *Electrochimica Acta* **36**, 1345.

Elder, J. W. 1965 *J. Fluid Mech.* **23**, 77.

Elder, J. W. 1966 *J. Fluid Mech.* **24**, 823.

Fusegi, T., Hyun, J. M. & Kuwahara, K. 1991 *Intl J. Heat and Mass Transfer* (to appear).

Gebhart, B., Jaluria, Y., Mahajan, R. L. & Sammakia, B. 1988 *Buoyancy Induced Flow and Transport.* Springer.

Gill, A. E. 1966 *J. Fluid Mech.* **26**, 515.

Gu, H., Nguyen, T. V. & White, R. E. 1987 *J. Electrochem. Soc.* **134**, 2953.

Hine, F. 1985 *Electrode Processes and Electrochemical Engineering.* Plenum.

Hyun, J. M. 1984 *Intl J. Heat Mass Transfer* **27**, 1986.

Hyun, J. M. 1985*a* *J. Phys. Soc. Japan* **54**, 942.

Hyun, J. M. 1985*b* *Intl J. Heat Mass Transfer* **29**, 499.

Ivey, G. N. 1984 *J. Fluid Mech.* **144**, 389.

Jischke, M. C. & Doty, R. T. 1975 *J. Fluid Mech.* **71**, 729.

Johansson, C. 1987 A new method for computing unsteady two-dimensional convective-diffusive mass transport. Licentiate thesis, *Internal Rep.* 87-1, Dep. of Comp. Sci., University of Uppsala.

Karlsson, R. I., Alavyoon, F. & Eklund, A. 1990 *Laser Anemometry – Proc. 3rd Intl Conf.*, p. 329. Springer.

Kimura, S. & Bejan, A. 1984 *Trans. ASME* C: *J. Heat Transfer* **106**, 99.

Kuiken, H. K. 1978 *J. Engng Maths* **2**, 353.

Le Févre, E. J. 1957 In *Proc. IXth IUTAM Congress, Brussels*, p. 168.

Newman, J. 1973 *Electrochemical Systems.* Prentice.

OSTRACH, S. 1963 *NACA* Rep. 1111.

PATTERSON, J. 1983 *Trans. ASME* **106**, 104.

PATTERSON, J. & IMBERGER, J. 1980 *J. Fluid Mech.* **100**, 65.

PRANDTL, L. 1952 *Essentials of Fluid Dynamics*. Blackie & Son.

RAHM, L. 1985 *Mathematical Modelling* **6**, 19.

RAHM, L. & WALIN, G. 1979*a* *J. Fluid Mech.* **90**, 315.

RAHM, L. & WALIN, G. 1979*b* *Astrophysics. Fluid Dyn.* **13**, 51.

SAKURAI, T. & MATSUDA, T. 1972 *J. Fluid Mech.* **54**, 417.

SCHLADOW, S. G. 1990 *J. Fluid Mech.* **213**, 589.

SMITH, S. H. 1981 *SIAM J. Appl. Maths* **40**, 78.

VAHL DAVIS, G. DE 1968 *Intl J. Heat Mass Transfer* **11**, 1675.

VERONIS, G. 1967*a* *Tellus* **19**, 326.

VERONIS, G. 1967*b* *Tellus* **19**, 620.

VERONIS, G. 1970 *Ann. Rev. Fluid Mech.* **2**, 37.

WALIN, G. 1971 *J. Fluid Mech.* **48**, 647.